České vysoké učení technické v Praze
Fakulta elektrotechnická

Czech Technical University in Prague
Faculty of Electrical Engineering

Ing. Tomáš Pajdla, Ph.D.

Globální optimalizace v kalibraci kamer a robotů

Global Optimization in Camera and Robot Calibration

Summary

Estimating calibration parameters of cameras on robots is an important problem that has to be solved in almost every practical system in robotics and computer vision. In many situations, it is desirable to find a globally optimal solution to achieve best result possible or to benchmark other, more efficient but suboptimal methods. We show how to formulate some of the fundamental camera and camera-robot calibration problems in order to solve them using methods from global polynomial optimization.

Souhrn

V praktických úlohách počítačového vidění a robotiky je třeba kalibrovat parametry kamer, které jsou neseny robotem. Často je velmi užitečné najít globálně optimální řešení, aby byl dosažen nejlepší možný výsledek, nebo aby bylo možno vyhodnotit kvalitu jiných efektivnějších ale sub-optimálních přístupů. Ukážeme, jak formulovat některé důležité problémy kalibrace kamer a kamer nesených roboty a jak je řešit metodami globální polynomiální optimalizace.

Klíčová slova: Kalibrace kamer a robotů, globální optimalizace

Keywords: Camera and robot calibration, global optimization

Contents

Chapter 1

Introduction

Cameras are often mounted on moving mechanisms, Fig. 1.1, to control the motion of the mechanisms by observations in images. For instance, image measurements guide robot tools, e.g. welding laser beam or grippers, to desired position and driving assistance systems "drive" cars based on traffic situation recognized in images, Figure 1.2.

In order to connect image measurements to natural coordinate systems of robots and cars, it is necessary to (1) calibrate camera projection [1] and to (2) calibrate camera pose w.r.t. a natural coordinate system of a mechanism [2]. It is customary to denote the first task as *camera calibration* and the second task as *hand-eye calibration*, Fig. 1.3.

We present several variations of camera calibration and hand-eye calibration problems that benefit from employing global optimization techniques.

1.1 Camera calibration

A convenient camera model [1, 3], which works for most cameras,

$$\mathtt{u} = \mathcal{A}(\mathcal{D}(\mathcal{P}(\mathtt{Y}))), \quad \mathcal{P}\left(\begin{bmatrix} x \\ y \\ z \end{bmatrix}\right) = \begin{bmatrix} x/z \\ y/z \end{bmatrix}, \quad \mathcal{A}(\mathtt{v}) = \mathtt{A}\,\mathtt{v} + \mathtt{b} \tag{1.1}$$

projects a 3D point $\mathtt{Y} \in \mathbb{R}^3$ from the camera Cartesian coordinate system to an image point $\mathtt{u} \in \mathbb{R}^2$ by a composition of perspective projection $\mathcal{P} : \mathbb{R}^3 \to \mathbb{R}^2$, lens non-linearity mapping $\mathcal{D} : \mathbb{R}^2 \to \mathbb{R}^2$ and affine mapping $\mathcal{A} : \mathbb{R}^2 \to \mathbb{R}^2$ choosing image coordinate system, Fig. 1.3(a). Functions $\mathcal{P}$ and $\mathcal{A}$ are standard, with parameters $\mathtt{A} \in \mathbb{R}^{2\times 2}$, $\mathtt{b} \in \mathbb{R}^2$. There are many different possibilities how to choose function $\mathcal{D}$. A standard model [4] is obtained by combining radial distortion based on

(a) (b) (c)

Figure 1.1: (a) Canon EOS with Sigma 180° view angle lens mounted on an industrial robot. (b) ASUS Action 3D sensors, consisting of perspective cameras and IR projectors, mounted on a two-armed industrial robot. (c) An omnidirectional catadioptric camera with 100° × 360° view angle mounted on Mercedes-Benz Actros vehicle. (By courtesy of CLOPEMA project and Daimler AG)

rational polynomial model [5] with tangential distortion [6]

$$\begin{aligned} \mathcal{D}\left(\begin{bmatrix} u \\ v \end{bmatrix}\right) &= L(r)\begin{bmatrix} u \\ v \end{bmatrix} + \begin{bmatrix} 2p_7 u\,v + p_8(r^2+u^2) \\ p_7(r^2+v^2) + 2p_8 u\,v \end{bmatrix} \qquad (1.2) \\ L(r) &= \frac{f(r)}{g(r)} = \frac{1+p_1 r + p_2 r^2 + p_3 r^3}{1+p_4 r + p_5 k^2 + p_6 r^3} \quad \text{with} \quad r = u^2+v^2 \end{aligned}$$

Camera calibration identifies parameters $\mathtt{A}, \mathtt{b}, p_i$ from measured 3D points $\mathtt{Y}$ and their images $\mathtt{u}$.

There is an extensive literature on camera calibration. Majority of works follows the standard procedure [7, 1, 8], which first estimates an initial solution by a suboptimal, often linearized, method and then refines it by a local optimization [9]. We will first show that this approach may lead to serious problems when using rational polynomial models and secondly how to avoid them by using global polynomial optimization [10].

1.2 Hand-Eye and Robot-World calibration

Consider a calibrated camera is mounted on a rigid body B, which is a part of a mechanism, Fig. 1.3(b). The unknown relation between the camera and body B is modeled by transformation $\mathtt{X} = \left[\mathtt{R}, \mathtt{t}\,;\, 0^\top, 1\right]$ with rotation $\mathtt{R} \in \mathbb{R}^{3\times 3}$ and translation $\mathtt{t} \in \mathbb{R}^3$. Analogically, the relationship between the base coordinate system of the manipulator and the world coordinate system is captured by transformation $\mathtt{Z}$. Transformations $\mathtt{B}_i$, which relate the coordinate system attached to body B to the base coordinate system, are available from the control system of the mechanism. Analogically, transformations $\mathtt{A}_i$, which relate the

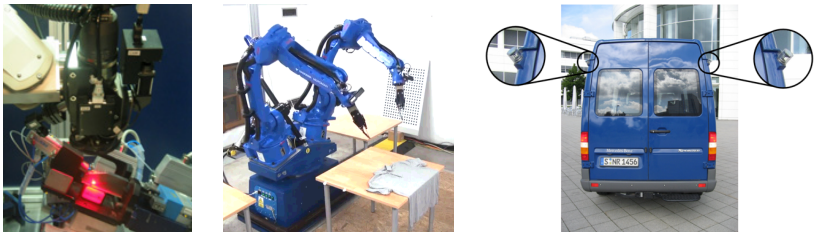

(a) (b) (c)

Figure 1.2: (a) A laser welding application by Mitsubishi Melfa robot carrying a measurement camera and a welding laser. (b) Robotic cloth manipulation by a pair of Motoman robots guided by Action 3D sensors. (c) Omnidirectional cameras mounted on Mercedes Sprinter Car. (By courtesy of Neovision s.r.o., Daimler AG and CLOPEMA project)

camera coordinate system to the world coordinate system, are available as a side-product of camera calibration or from a 3D reconstruction by Structure from Motion [11].

For every two different poses of the manipulator $\mathtt{B}'_{i1}, \mathtt{B}'_{i2}$ and the corresponding camera poses $\mathtt{A}'_{i1}, \mathtt{A}'_{i2}$, we can formulate *Hand-Eye calibration* equations

$$\mathtt{A}_i\mathtt{X} = \mathtt{X}\,\mathtt{B}_i \quad \text{with} \quad \mathtt{A}_i = \mathtt{A}'^{-1}_{i2}\mathtt{A}'_{i1},\ \mathtt{B}_i = \mathtt{B}'^{-1}_{i2}\mathtt{B}'_{i1} \tag{1.3}$$

and *Hand-Eye and Robot-World calibration* equations

$$\mathtt{A}'_i\mathtt{X} = \mathtt{Z}\,\mathtt{B}'_i \tag{1.4}$$

It theory [12], three general poses suffice to solve for $\mathtt{X}$ from Hand-Eye calibration equations but in practice more poses are used and computing $\mathtt{X}, \mathtt{Z}$ is posed as an optimization problem [12].

There is an extensive literature on Hand-Eye and Robot-World calibration. Many works, e.g. [13, 2, 14], first estimate an initial solution by a suboptimal method and then refine it by a local optimization. Such approach is often useful in practice but may miss the global optimum if the initialization fails. They also often first solve for rotation $\mathtt{R}$ only and then compute translation $\mathtt{t}$. It leads to a simpler problem but it is known to suffer from larger errors [15] compared to optimizing $\mathtt{R}, \mathtt{t}$ together. Other methods avoid Hand-Eye calibration equations but (often globally) optimize image reprojection errors [16, 17, 11, 18, 19, 20]. This approach fails when image measurements are not available. Moreover, many of these methods are based on Branch and Bound techniques, which become computationally expensive when estimating more

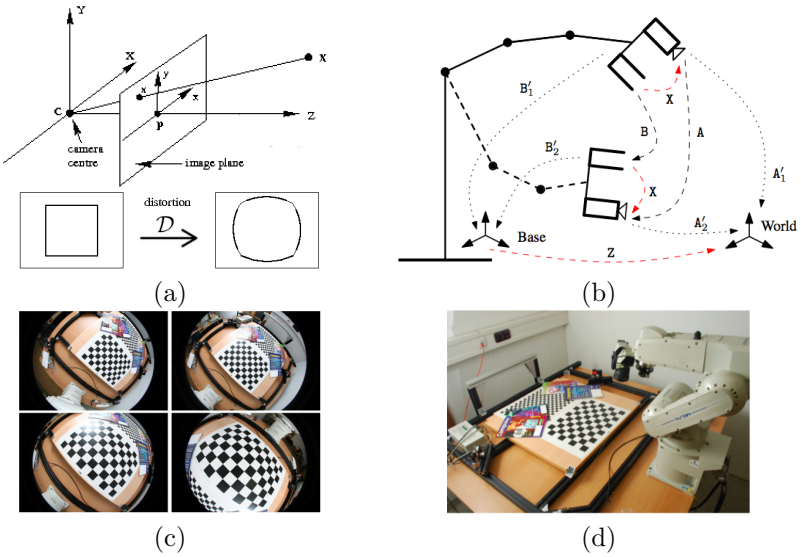

Figure 1.3: (a) Camera calibration identifies parameters of the camera projection function model in Eqn. 1.1. (b) Hand-Eye calibration identifies transformation $\mathtt{X}$, which relates the camera to the mechanism and, optionally, also transformation $\mathtt{Z}$, which relates the mechanism to a world coordinate system. (c) Camera is calibrated by observing a known (planar) calibration target from several (unknown) positions. (d) Poses $\mathtt{A}_i$ of a calibrated camera w.r.t. a world coordinate system can be computed from observing a known (planar) calibration target.

than three parameters. Other "globally optimal" methods [21, 22, 23] either do not enforce $\mathtt{R}$ to be a valid rotation and require another correction step afterwards, which does not guarantee any optimality, or use objective functions based on some algebraic error, which may be geometrically meaningless [24, 25]. Finally, [26] formulates the Eye-Hand calibration problem as an algebraic problem but can't use the measured orientation of body B.

We will show that Hand-Eye and Robot-World calibration problems can be solved optimally [27, 28] for meaningful errors using polynomial optimization.

Chapter 2

Polynomial optimization and Linear Matrix Inequalities (LMI)

2.1 LMI hierarchy of convex relaxations

Consider multivariate polynomials $p_i(\mathbf{x}) \in \mathbb{R}[\mathbf{x}]$, $i = 0, \ldots, \ell$ in $\mathbf{x} = (x_1, \ldots, x_m)^\top \in \mathbb{R}^m$. Multivariate polynomial optimization can be stated as follows

$$\begin{array}{rl} \text{minimize} & p_0(\mathbf{x}) \\ \text{subject to} & p_i(\mathbf{x}) \geqslant 0,\ i = 1, \ldots, \ell, \\ \text{where} & \mathbf{x} = (x_1, x_2, \ldots, x_m)^\top \in R^m, \\ & p_0(\mathbf{x}), p_i(\mathbf{x}) \in \mathbb{R}[\mathbf{x}]. \end{array} \tag{2.1}$$

This is in general a non-convex problem with many local minima. In theory, it can be handled using tools of elementary calculus but finding the global minimizer $\mathbf{x}^*$ is, in general, an NP-hard problem [29]. Using Putinar's results [30], Lasserre showed [31] that one can construct a (Lasserre's LMI) hierarchy of convex relaxations $\mathcal{P}_1, \mathcal{P}_2, \ldots$ that produces a monotonically non-decreasing sequence of lower bounds on Problem 2.1 over a semi-algebraic set $S = \{\mathbf{x} \in \mathbb{R}^m \,|\, p_i(\mathbf{x}) \geqslant 0, i = 1, \ldots, \ell\}$. The sequence converges to the global minimum. Moreover, the series of the respective global optimizers $\mathbf{x}_1^*, \mathbf{x}_2^*, \ldots$ of problems $\mathcal{P}_1, \mathcal{P}_2, \ldots$ asymptotically converges to $\mathbf{x}^*$, $\lim_{i\to\infty} \mathbf{x}_i^* = \mathbf{x}^*$, and that under mild conditions global optimality of a relaxation can be detected and the global minimizers can be extracted by linear algebra from the solutions of the relaxation. Practically, $(\mathbf{x}_i^*)_{i\in\mathbb{N}}$ converges to $\mathbf{x}^*$ in finitely many steps, *i.e.*, there exists $j \in \mathbb{N}$, such that $\mathbf{x}_j^* = \mathbf{x}^*$.

Consider the linearization operator $L_{\mathbf{y}} \colon \mathbb{R}[\mathbf{x}] \to \mathbb{R}[\mathbf{y}]$ which takes a polynomial $p(\mathbf{x})$ and substitutes a new variable $y_\alpha \in \mathbb{R}$ for every monomial $\mathbf{x}^\alpha = x_1^{k_1} x_2^{k_2} \ldots x_m^{k_m}$. First, the LMI relaxation $\mathcal{P}_\delta$ of order δ is built by linearizing all monomials $\mathbf{x}^\alpha$ of the objective function p_0 up to degree 2δ, *i.e.*, $k_1 + k_2 + \cdots + k_m \leqslant 2\delta$. If the objective function contains monomials of a higher degree, one has to start with a relax-

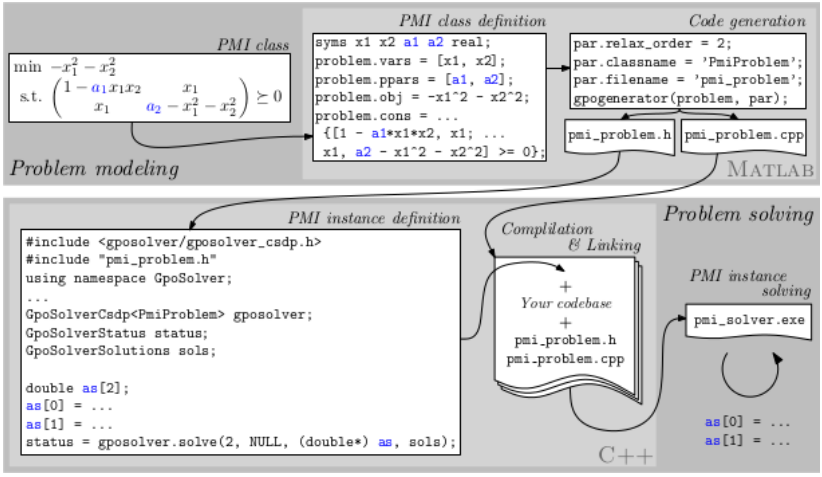

Figure 2.1: GpoSolver workflow. The workflow is divided into the problem modeling phase and the problem solving phase. In the next figure, the problem parameters are denoted in blue. The concrete values of these parameters are not determined until the problem solving phase. There, the parameters can be easily updated and different problem instances can be conveniently solved.

ation of a higher order. Next, let $\mathbf{v}_\delta(\mathbf{x})$ be the vector of all monomials up to degree δ. The semialgebraic set S is relaxed by introducing ℓ LMI constraints $L_\mathbf{y}(p_i(\mathbf{x})\mathbf{v}_{\delta-1}(\mathbf{x})\mathbf{v}_{\delta-1}(\mathbf{x})^\top) \succeq 0$ ("$\mathtt{M} \succeq 0$" stands for "$\mathtt{M}$ is positive semidefinite matrix"). Finally, we add the so-called LMI moment matrix constraint $L_\mathbf{y}(\mathbf{v}_\delta(\mathbf{x})\mathbf{v}_\delta(\mathbf{x})^\top) \succeq 0$. Formally, the LMI relaxation $\mathcal{P}_\delta$ of order δ can be written as

$$\begin{array}{ll} \text{minimize} & L_\mathbf{y}(p_0(\mathbf{x})) \\ \text{subject to} & L_\mathbf{y}(p_i(\mathbf{x})\mathbf{v}_{\delta-1}(\mathbf{x})\mathbf{v}_{\delta-1}(\mathbf{x})^\top) \succeq 0,\ i = 1, \ldots, \ell, \\ & L_\mathbf{y}(\mathbf{v}_\delta(\mathbf{x})\mathbf{v}_\delta(\mathbf{x})^\top) \succeq 0. \end{array} \tag{2.2}$$

Since there are exactly $d = \binom{m+2\delta}{m}$ monomials in $\mathbf{x} \in \mathbb{R}^m$ up to degree 2δ, SDP Problem 2.2 will have $\mathbf{y} \in \mathbb{R}^d$ linear variables.

2.2 GpoSolver toolbox

From a practical point of view, it is extremely important that the relaxations $\mathcal{P}_1, \mathcal{P}_2, \ldots$ can be formulated as semi-definite programs (SDP) solvable by any convenient SDP solver. Software implementations of LMI relaxations can be found e.g. in Matlab toolboxes GloptiPoly [32]

and YALMIP [33]. Matlab language is very convenient for modelling polynomial problems but it is a too heavy tool when an efficient "production" implementation is required. Our GpoSolver [34] provides a Matlab-based problem modelling toolbox supplemented by a problem-solving back end in a form of a C++ template library, Fig. 2.1. Once a problem is conveniently modelled and parametrized in Matlab, a C++ class is automatically generated by GpoSolver. This class can be easily included into an existing codebase and used to solve different instances of the problem based on the supplied parameters.

2.3 Non-negative polynomials

A polynomial $p(x) \in \mathbb{R}_n[x]$ of degree $n \in \mathbb{N}$ can be written as $p(x) = p_n x^n + p_{n-1}x^{n-1} + \cdots + p_1 x + p_0 = \mathbf{p}^\top \mathbf{v}_n(x)$ with a coefficient vector $\mathbf{p} = (p_0, p_1, \ldots, p_n)^\top \in \mathbb{R}^{n+1}$ and the canonical monomial basis $\mathbf{v}_n(x) = (1, x, x^2, \ldots, x^n)^\top$. A polynomial $q(x) \in \mathbb{R}_{2n}[x]$ can be written as

$$q(x) = \mathbf{v}_n^\top(x)\, \mathtt{Q}\, \mathbf{v}_n(x) \tag{2.3}$$

with a symmetric *Gram matrix* matrix $\mathtt{Q} \in \mathbb{R}^{n+1\times n+1}$ [35].

Markov-Lukacs theorem [36] characterizes polynomials that are non-negative on a real interval $[\alpha, \beta]$, $\alpha < \beta$, using positive semidefinite Gram matrices $\mathtt{S}, \mathtt{T}$: A polynomial $p(x) \in \mathbb{R}[x]$ is non-negative on $[\alpha, \beta]$ if and only if (i) for $\deg p(x) = 2n$ it can be written as $p(x) = s(x) + (x-\alpha)(\beta - x)t(x)$ with $s(x) = \mathbf{v}_n^\top(x)\, \mathtt{S}\, \mathbf{v}_n(x)$, $t(x) = \mathbf{v}_{n-1}^\top(x)\, \mathtt{T}\, \mathbf{v}_{n-1}(x)$ or (ii) for $\deg p(x) = 2n+1$ it can be written as $p(x) = (x-\alpha)s(x) + (\beta - x)t(x)$ with $s(x) = \mathbf{v}_n^\top(x)\, \mathtt{S}\, \mathbf{v}_n(x)$, $t(x) = \mathbf{v}_n^\top(x)\, \mathtt{T}\, \mathbf{v}_n(x)$.

Chapter 3

Camera calibration

Figure 3.1(a) Top shows that using the standard model in Eqn. 1.2 and a standard calibration procedure implemented, e.g., in [4], leads to serious problems. The figure shows image undistorted [1] by inverting function $\mathcal{D}$ for estimated parameters. Image center, which was covered by calibration data, is undistorted correctly. However, image undistortion is completely wrong further from the center in the area where the calibration model extrapolates. The circular artifact is caused by "zero division" effect in radial distortion function $L(r)$. The function is unnecessarily complex for this particular camera and thus the numerator $f(r)$ and denominator $g(r)$ contain linear factors that almost cancel. The ratio of the linear factors is thus equal to one almost everywhere except for a very narrow area where $f(r)$ is small but non-zero and $g(r)$ goes to zero. In general, it is desirable and possible to avoid the "zero division" artifact. Let us show how this can be achieved when using polynomial matrix inequalities (PMI) and how to estimate parameters of $L(r)$ subject to PMI constraints using SDP [10].

The artifact is generated due to wrong $L(r)$. Other calibration parameters, even when estimated with wrong $L(r)$, are estimated almost correctly by the classical calibration approach. Therefore, better calibration can be obtained by (1) initializing all parameters by the classical method, then (2) optimizing parameters of $L(r)$ subject to PMI constraints, and (3) optimizing other parameters by a local optimization with $L(r)$ fixed. If necessary, steps (2) and (3) can be repeated until convergence.

To correct $L(r)$, we have to avoid a common root of the polynomials $f(r)$ and $g(r)$ on the field of view interval $[0, \bar{r}]$, i.e. to enforce at least one on them to have no root. We enforce $g(r) > 0$, i.e. $g(r) - \epsilon \geqslant 0$, with a small $\epsilon > 0$ on $[0, \bar{r}]$.

By applying Markov-Lukacs theorem to the above, we get

$$g(r)-\epsilon = 1-\epsilon+p_4 r+p_5 r^2+p_6 r^3 = \boldsymbol{v}_1(r)^\top \mathtt{S}_1 \boldsymbol{v}_1(r)+(\bar{r}-r)\, \boldsymbol{v}_1(r)^\top \mathtt{T}_1 \boldsymbol{v}_1(r)$$

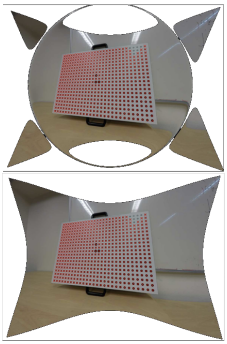

(a)

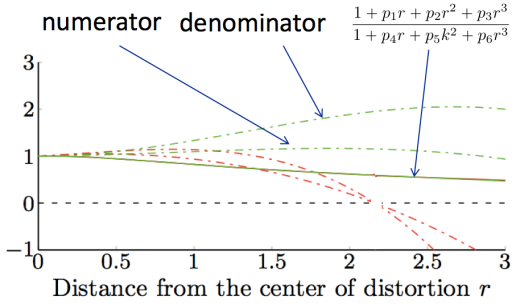

(b)

Figure 3.1: (a) Top. An image undistorted using camera parameters calibrated by a standard initialization + local optimization paradigm. (a) Bottom: The image undistorted with constraining the model to be positive on the field of view. (b) The circular artifact in (a) Top is caused by inexact cancellation of redundant terms in the numerator and denominator of the radial distortion part of the model (red curves). Green curves show numerator and denominator constrained to be positive on the whole field of view.

with $\mathtt{S}_1, \mathtt{T}_1 \in \mathbb{R}^{2\times 2}, \mathtt{S}_1, \mathtt{T}_1 \succeq 0$. Having all other calibration parameters fixed, it suffices to minimize $\sum_i \left\| g(r) \begin{bmatrix} \hat{u}_i \\ \hat{v}_i \end{bmatrix} - f(r) \begin{bmatrix} u_i \\ v_i \end{bmatrix} \right\|^2 = \mathtt{p}^\top \mathtt{L}^\top \mathtt{L}\, \mathtt{p} + \mathtt{m}^\top \mathtt{p} + c$ where matrix $\mathtt{L}$, vector $\mathtt{m}$ and scalar c depend on image measurements u_i, v_i and their estimate $\hat{u}_i, \hat{v}_i$ obtained using other fixed parameters. Vector $\mathtt{p}$ of parameters is computed from p_1, p_2, p_3 and elements of $\mathtt{S}_1, \mathtt{T}_1$ [10]. Using Schur complement and slack variable γ, we get a radial distortion calibration

$$\begin{aligned} &\text{minimize} \quad \gamma \\ &\text{subject to} \quad \mathtt{F} = \begin{bmatrix} \mathtt{I} & \mathtt{L}\,\mathtt{p} \\ \mathtt{p}^\top \mathtt{L}^\top & -\mathtt{m}^\top \mathtt{p} - c + \gamma \end{bmatrix} \succeq 0,\ \mathtt{S}_1 \succeq 0,\ \mathtt{T}_1 \succeq 0. \end{aligned}$$

which is an LMI program in 9 variables $\gamma, s_{11}, s_{12}, s_{13}, t_{12}, t_{13}, p_1, p_2, p_3$. This can be solved by GpoSolver [34]. Additional constraints on calibration function, e.g. requiring the radial distortion to be of pincushion type, leads to a more difficult PMI problem that requires additional LMI relaxations [10].

Chapter 4

Hand-Eye and Robot-World calibration

Consider a mechanism with a camera mounted on one of its rigid bodies B and positioned into n different general poses out of which k pairs are formed. Equations 1.3 and 1.4 can't be exactly satisfied if there is noise in measurements $\mathtt{A}'_i, \mathtt{B}'_i$. We therefore pose the calibration as minimization problems

$$\min_{\mathtt{X}\in SE(3)} \sum_{i=1}^{k} \|\mathtt{A}_i\mathtt{X} - \mathtt{X}\mathtt{B}_i\|^2 \quad \text{or} \quad \min_{\mathtt{X},\mathtt{Z}\in SE(3)} \sum_{i=1}^{n} \|\mathtt{A}'_i\mathtt{X} - \mathtt{Z}\,\mathtt{B}'_i\|^2$$

with Frobenius norm $\|.\|$. Special Euclidean group $SE(3)$ consists of matrices $\left[\mathtt{R}, \mathtt{t}\,;\, \mathtt{0}^\top, 1\right]$ with a 3×3 rotation $\mathtt{R}$ and a translation $\mathtt{t} \in \mathbb{R}^3$. Alternatively, almost equivalent formulation can be obtained in dual quaternions [27]. We will demonstrate the approach using Frobenius norm formulation for Hand-Eye and Robot-World calibration problem. There are many ways how to constrain $\mathtt{X}$ and $\mathtt{Z}$ to be in $SE(3)$. We will show quaternion parameterization here. Other parameterizations have been studied in [27]. Hence, matrices $\mathtt{X}(\mathtt{q}_\mathtt{X}, \mathtt{t}_\mathtt{X}) = \left[\mathtt{R}(\mathtt{q}_\mathtt{X}), \mathtt{t}_\mathtt{X}\,;\, \mathtt{0}^\top, 1\right]$, $\mathtt{Z}(\mathtt{q}_\mathtt{Z}, \mathtt{t}_\mathtt{Z}) = \left[\mathtt{R}(\mathtt{q}_\mathtt{Z}), \mathtt{t}_\mathtt{Z}\,;\, \mathtt{0}^\top, 1\right]$ are parameterized by 7 parameters $\mathtt{q} \in \mathbb{R}^4$, $\|\mathtt{q}\|^2 = 1$ and $\mathtt{t} \in \mathtt{R}^3$ with $\mathtt{R}(\mathtt{q}) = \begin{bmatrix} q_1^2+q_2^2-q_3^2-2q_4^2 & 2q_2q_3-2q_4q_1 & 2q_2q_4+2q_3q_1 \\ 2q_2q_3+2q_4q_1 & q_1^2-q_2^2+q_3^2-q_4^2 & 2q_3q_4-2q_2q_1 \\ 2q_2q_4-2q_3q_1 & 2q_3q_4+2q_2q_1 & q_1^2-q_2^2-q_3^2+2q_4^2 \end{bmatrix}$. To avoid most of double solutions due to $\mathtt{R}(\mathtt{q}) = \mathtt{R}(-\mathtt{q})$, we can add constraint $\mathtt{q}_{\mathtt{X}1}, \mathtt{q}_{\mathtt{Z}1} \geqslant 0$. It leaves double solutions only for rotations by 180 degrees, which almost never occur.

We are thus getting the following optimization problem

$$\begin{array}{rl} \text{minimize} & f(\mathtt{q}_\mathtt{X}, \mathtt{t}_\mathtt{X}, \mathtt{q}_\mathtt{Z}, \mathtt{t}_\mathtt{Z}) = \sum_{i=1}^{n} \|\mathtt{A}'_i\mathtt{X}(\mathtt{q}_\mathtt{X}, \mathtt{t}_\mathtt{X}) - \mathtt{Z}(\mathtt{q}_\mathtt{Z}, \mathtt{t}_\mathtt{Z})\mathtt{B}'_i\|^2 \\ \text{subject to} & \mathtt{q}_\mathtt{X}^\top \mathtt{q}_\mathtt{X} = 1,\ \mathtt{q}_{\mathtt{X}1} \geqslant 0,\ \mathtt{q}_\mathtt{Z}^\top \mathtt{q}_\mathtt{Z} = 1,\ \mathtt{q}_{\mathtt{Z}1} \geqslant 0, \\ & \mathtt{t}_\mathtt{X}^\top \mathtt{t}_\mathtt{X} \leqslant s_\mathtt{X},\ \mathtt{t}_\mathtt{Z}^\top \mathtt{t}_\mathtt{Z} \leqslant s_\mathtt{Z}. \end{array}$$

Objective function f is a polynomial of degree 4 and is composed of 209

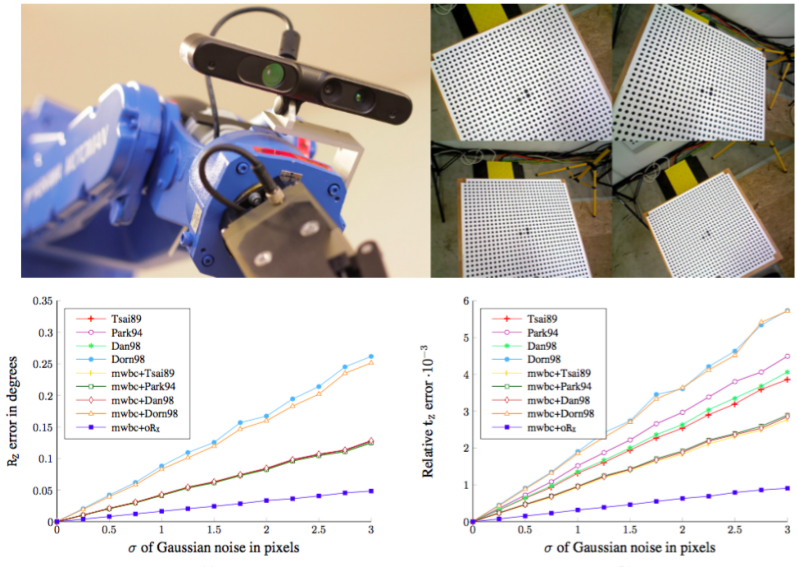

Figure 4.1: Top: Real experiments with Hand-Eye and Robot-World calibration were carried out on Motoman manipulator with Xtion 3D sensor comprising a calibrated perspective camera and a planar calibration target. Bottom: Robot-World calibration mwbc-* formulated in [28] achieved considerably more accurate estimates of robot pose than other methods.

monomials in 14 variables. GpoSolver [34] could not find any solution without constraining the length of translations by $\mathtt{t}_\mathtt{X}^\top \mathtt{t}_\mathtt{X} \leqslant s_\mathtt{X}, \mathtt{t}_\mathtt{Z}^\top \mathtt{t}_\mathtt{Z} \leqslant s_\mathtt{Z}$ for some parameters $s_\mathtt{X}, s_\mathtt{Z} \geqslant 0$. However, after adding the final constraints, GpoSolver was able to obtain and certify the global minimum.

In [28], yet another variation of the problem was studied. Assuming that Hand-Eye calibration $\mathtt{X}$ has already been recovered, e.g. by a Hand-Eye calibration from [27], it is possible to cast Robot-World calibration problem as a kind of the camera resectioning problem [1] in seven unknowns only when objective function minimizes the object space error. It turns out that the objective function is quadratic in $\mathtt{t}_\mathtt{Z}$ and thus optimal $\mathtt{t}_\mathtt{Z}$ can be written in a closed form for known $\mathtt{R}_\mathtt{Z}$. That reduces the number of parameters further to four. This reduction of the number of unknowns makes the problem tractable within LMI relaxation framework with one second order LMI relaxation. Fig. 4.1 Bottom shows that this approach outperforms alternative methods in accuracy.

References

[1] R. Hartley and A. Zisserman. *Multiple View Geometry in Computer Vision*. Cambridge, 2nd edition, 2003.

[2] F. Dornaika and R. Horaud. Simultaneous Robot-World and Hand-Eye calibration. *IEEE Trans. Robotics and Autom.*, 14(4):617–622, 1998.

[3] B. Micusik and T. Pajdla. Structure from motion with wide circular field of view cameras. *IEEE Trans. on PAMI*, 28(7):1135–1149, 2006.

[4] G. Bradski. OpenCV. *Dr. Dobb's Journal of Software Tools*, 2000.

[5] L. Ma, Y. Chen, and K. L. Moore. Rational radial distortion models of camera lenses with analytical solution for distortion correction. *I. J. Information Acquisition*, 1(2):135–147, 2004.

[6] Janne Heikkila. Geometric camera calibration using circular control points. *IEEE Trans. on PAMI*, 22(10):1066–1077, 2000.

[7] O. Faugeras. *Three-Dimensional Computer Vision*. MIT Press, 1993.

[8] Y. Ma, S. Soatto, J. Kosecka, and S. Shankar Sastry. *An invitation to 3-D vision: from images to geometric models*. Interdisciplinary applied mathematics. Springer, 2004.

[9] B. Triggs, P. F. McLauchlan, R. Hartley, and A. Fitzgibbon. Bundle adjustment - A modern synthesis. *Vision Algorithms: Theory and Practice*, Int. Workshop on Vision Algorithms, ICCV'99, pp. 298–372, 1999.

[10] J. Heller, D. Henrion, and T. Pajdla. Stable radial distortion calibration by polynomial matrix inequalities programming. *ACCV 2014: Asian Conference on Computer Vision*, vol. 9003 of *LNCS*, pp. 307–321, Springer, 2015.

[11] J. Heller, M. Havlena, A. Sugimoto, and T. Pajdla. Structure-from-motion based hand-eye calibration using l-∞ minimization. *CVPR 2011: IEEE Conf. on Computer Vision and Pattern Recognition*, pp. 3497–3503, 2011.

[12] Y.C. Shiu and S. Ahmad. Calibration of wrist-mounted robotic sensors by solving homogeneous transform equations of the form AX=XB. *IEEE Trans. on Robotics and Automation*, 5(1):16–29, 1989.

[13] H. Zhuang and Y. C. Shiu. A noise tolerant algorithm for wrist-mounted robotic sensor calibration with or without sensor orientation measurement. In *lEEE/RSJ Int. Conf. on Intelligent Robots and Systems*, vol. 2, pages 1095–1100, 1992.

[14] R. Horaud and F. Dornaika. Hand-eye calibration. *The International Journal of Robotics Research*, 14(3):195–210, 1995.

[15] H. H. Chen. A screw motion approach to uniqueness analysis of head-eye geometry. In *CVPR 1991: IEEE Conf. on Computer Vision and Pattern Recognition*, pp. 145–151, 1991.

[16] Y. Seo, Y.-J. Choi, and S. W. Lee. A branch-and-bound algorithm for globally optimal calibration of a camera-and-rotation-sensor system. In *ICCV 2009: IEEE Int. Conference on Computer Vision*, pp. 1173–1178, 2009.

[17] S.-J. Kim, M.-H. Jeong, J.-J. Lee, J.-Y. Lee, K.-G. Kim, B.-J. You, and S.-R. Oh. Robot head-eye calibration using the minimum variance method. *IEEE Int. Conference on Robotics and Biomimetics (ROBIO)*, pp. 1446–1451, 2010.

[18] J. Heller, M. Havlena, and T. Pajdla. A branch-and-bound algorithm for globally optimal hand-eye calibration. In *CVPR 2012: IEEE Conf. on Computer Vision and Pattern Recognition*, pp. 1608–1615, 2012.

[19] J. Heller, M. Havlena, and T. Pajdla. Globally optimal hand-eye calibration using branch-and-bound. *IEEE Trans. on PAMI*, 38(5): 1027-1033, 2016.

[20] T. Ruland, L. Kruger, and T. Pajdla. Globally optimal hand-eye calibration. *CVPR 2012: IEEE Conf. on Computer Vision and Pattern Recognition*, pp. 1035–1042, 2012.

[21] Zijian Zhao. Hand-eye calibration using convex optimization. *ICRA*, pp. 2947–2952, 2011.

[22] N. Andreff, R. Horaud, and B. Espiau. On-line hand-eye calibration. *Int. Conference on 3-D Digital Imaging and Modeling, 1999*, pp. 430–43,. IEEE, 1999.

[23] L. Wang, A. Li and D. Wu. Simultaneous robot-world and hand-eye calibration using dual-quaternions and Kronecker product. *International Journal of the Physical Sciences*, Vol. 5(10):pp. 1530–1536, 2010.

[24] K. Daniilidis and E. Bayro-Corrochano. The dual quaternion approach to hand-eye calibration. In *ICPR '96: Int. Conference on Pattern Recognition, Volume I*, pp. 318, IEEE, 1996.

[25] K. Daniilidis. Hand-eye calibration using dual quaternions. *International Journal of Robotics Research*, 18:286–298, 1998.

[26] Z. Kukelova, J. Heller, and T. Pajdla. Hand-eye calibration without hand orientation measurement using minimal solution. In *ACCV 2012: Asian Conference on Computer Vision*, vol. 7727 of *LNCS*, pp. 576–589, Springer, 2013.

[27] J. Heller, D. Henrion, and T. Pajdla. Hand-eye and robot-world calibration by global polynomial optimization. In *ICRA 2014: IEEE Int. Conference on Robotics and Automation*, pp. 3157–3164, 2014.

[28] J. Heller and T. Pajdla. World-Base calibration by global polynomial optimization. In *3DV 2014: 2nd International Conference on 3D Vision*, Vol. 1, pp. 593–600, 2014.

[29] K. G. Murty and S. N. Kabadi. Some NP-complete problems in quadratic and nonlinear programming. *Mathematical programming*, 39(2):117–129, 1987.

[30] M. Putinar. Positive polynomials on compact semi-algebraic sets. *Indiana University Mathematics Journal*, 42(3):969–984, 1993.

[31] J.-B. Lasserre. Global optimization with polynomials and the problem of moments. *SIAM Journal on Optimization*, 11:796–817, 2001.

[32] D. Henrion, J.-B. Lasserre, and J. Löfberg. Gloptipoly 3: moments, optimization and semidefinite programming. *Optimization Methods & Software*, 24(4-5):761–779, 2009.

[33] J. Löfberg. YALMIP: A toolbox for modeling and optimization in MATLAB. In *CACSD Conference*, Taipei, Taiwan, 2004.

[34] J. Heller and T. Pajdla. GpoSolver: a matlab/c++ toolbox for global polynomial optimization. *Optimization Methods and Software*, 31(2):405–434, 2016.

[35] M.-D. Choi, T. Y. Lam, and B. Reznick. Sums of squares of real polynomials. *Proc. of Symposia in Pure Mathematics*, Vol. 58, pp. 103–126. American Mathematical Society, 1995.

[36] Y. Nesterov. Squared functional systems and optimization problems. In *High performance optimization*, pp. 405–440. Springer, 2000.

Ing. Tomáš Pajdla, Ph.D.

Born on May 10, 1969 in Prague, Czech Republic

1992	Ing. in Electrical Engineering, CTU in Prague
2003	Ph.D. in Electrical Engineering, CTU in Prague
1994—1995	Research Assistant, Katholieke Universiteit Leuven
1995—now	Assistant Professor, FEE, CTU in Prague
1996—2015	Partner and Chief of R&D in Neovision s.r.o.
1998/10-12	Visiting Researcher, TU Wien
2009/09	Visiting Researcher, Australian National University
2014/12-01	Visiting Researcher, NII Tokyo
2014—now	Distinguished Researcher, CIIRC, CTU in Prague
2015—now	Visiting Associate Professor, NII Tokyo

Research T. Pajdla works in Computer Vision, Robotics and Machine Learning including, and in particular in geometry, algebra and optimization of computer vision and robotics, 3D reconstruction from images, visual object recognition, and image based localization.

Publications He published more than research 100 works: 15 works in impacted journals (IEEE PAMI, IJCV, CVIU), 38 works in highly selective conferences (ICCV, CVPR, ECCV), and other works in MVA, ACCV, BMVC, OAGM, OMNIVIS, CVWW, and EPSC. He has h-index 14 and 1416 citations by Thomson WOS and h-index 42 and 9970 citations by Google Scholar.

Prizes He received prizes for results at OAGM 1998, BMVC 2002, OAGM 2013, and ACCV 2014. Theses of his students received prizes from Porsche (2009), Czech Society of Cybernetics and Informatics (2012, 2013) and the European Research Consortium for Informatics and Mathematics (2015).

Teaching He teaches "Geometry of Computer Vision and Graphics" and "Advanced Robotics" at the FEE of the CTU in Prague and at the Faculty of Mathematics and Physics of Charles University. He helped to build PhD course "Mathematics for Cybernetics" and contributed to textbook 16.

Students He supervised and co-supervised 10 Ph.D. and more than 30 MSc. and BSc. students. Many of them continued their careers, e.g., at the University of Oxford, ETH Zurich, Stanford University, INRIA/ENS, TU Delft, AIT Vienna and CTU in Prague.

Research & development projects He has been responsible investigator of 8 EU FP5/6/7 & H2020 projects at the CTU in Prague and

was a principal investigator of 3 projects from the Grant Agency and the Technology Agency of the Czech Republic. He lead R&D projects for Daimler, Intel, Leica Hexagon, Neovision, AZOS, Zentity, Gisat and Magik-Eye.

Editorial boards & conference organization He is at editorial boards of IEEE Transactions on Pattern Analysis and Machine Intelligence, Computer Vision and Image Understanding, Foundations and Trends in Computer Graphics and Vision. He was a Program Chair of the European Conference on Computer Vision 2004 and 2014 and area chair/program committee member/organizer at more than 30 ICCV, CVPR, ECCV, ACCV, BMVC, OMNIVIS, CVVT conferences and workshops.

Committees He participated in 12 PhD defense committees at U of Oxford, ANU, INP Grenoble, Dublin City University, EPFL Lausanne, INSA Lyon, U of Linkoping, EP ParisTech, Lund University and TU Wien. He is a member of the Panel Nr. 7-Mathematical Sciences of the Research, Development and Innovation Council of the Czech Republic.

Selected publications

1. T. Pajdla. Stereo with oblique cameras. International Journal of Computer Vision, 47(1-3): 161-170. 2002
2. T. Svoboda, T. Pajdla. Epipolar geometry for central catadioptric cameras. International Journal of Computer Vision, 49(1): 23-37. 2002.
3. P. Krsek, T. Pajdla, V. Hlavac. Differential invariants as the base of triangulated surface registration. Computer Vision and Image Understanding, 87(1): 27- 38. 2002.
4. T. Werner, T. Pajdla, V. Hlavac, A. Leonardis, M. Matousek. Selection of reference images for image-based scene representations. Computing, 68(2): 163-180. 2002.
5. J. Matas, O. Chum, M .Urban, T. Pajdla. Robust wide-baseline stereo from maximally stable extremal regions. Image and Vision Computing, 22(10): 761-767. 2004.
6. O. Chum, T. Pajdla, P. Sturm. The geometric error for homographies. Computer Vision and Image Understanding, 97(1): 86-102. 2005
7. B. Micusik, T. Pajdla. Structure from motion with wide circular field of view cameras. IEEE Trans. on Pattern Analysis and Machine Intelligence, 28(7): 1135–1149, July 2006.
8. T. Ehlgen, T. Pajdla, D. Ammon. Eliminating blind spots for assisted driving. IEEE Transactions on Intelligent Transportation Systems, 9(4): 657–665, December 2008.
9. Z. Kukelova, M. Byrod, K. Josephson, T. Pajdla, K. Astrom. Fast and robust numerical solutions to minimal problems for cameras with radial

distortion. Computer Vision and Image Understanding, 114(2):234–244, February 2010.

10. A. Torii, M. Havlena, T. Pajdla. Omnidirectional image stabilization for visual object recognition. International Journal of Computer Vision, 91(2): 157–174, January 2011.
11. Z. Kukelova, T. Pajdla. A minimal solution to radial distortion autocalibration. IEEE Trans. on Pattern Analysis and Machine Intelligence, 33(12): 2410–2422, December 2011.
12. Z. Kukelova, M. Bujnak, T. Pajdla. Polynomial eigenvalue solutions to minimal problems in computer vision. IEEE Trans. on Pattern Analysis and Machine Intelligence, 34(7):1381–1393, July 2012.
13. D. Weinshall, A. Zweig, H. Hermansky, S. Kombrink, F.W. Ohl, J. Anemuller, J-H. Bach, L. Van Gool, F. Nater, T. Pajdla, M. Havlena, M. Pavel. Beyond novelty detection: Incongruent events, when general and specific classifiers disagree. IEEE Trans. on Pattern Analysis and Machine Intelligence, 34(10):1886–1901, October 2012.
14. A. Torii, J. Sivic, M. Okutomi, T. Pajdla. Visual place recognition with repetitive structures visual place recognition with repetitive structures. IEEE Trans. on Pattern Analysis and Machine Intelligence, 37(11):2346–2359, 2015.
15. J. Heller, M. Havlena, T. Pajdla. Globally optimal hand-eye calibration using branch-and-bound. IEEE Trans. on Pattern Analysis and Machine Intelligence, 2015.
16. P. Pták, T. Pajdla. Některé matematické struktury používané v kybernetice. FEL ČVUT, Praha, 2008.